Exchange biasing and magnetic properties of partially and fully oxidized colloidal cobalt nanoparticles

Joseph B. Tracy, Dirk N. Weiss, Dmitry P. Dinega, and Moungi G. Bawendi*
Department of Chemistry, Massachusetts Institute of Technology, Cambridge, Massachusetts 02139, USA
(Received 24 October 2004; revised manuscript received 23 May 2005; published 2 August 2005)

Colloidal magnetic nanoparticles (NPs) have been applied in magnetic separations, in medicine and in biochemistry. They are also potentially applicable in magnetic recording media. In this paper, we report a systematic investigation of the magnetic properties of colloidal Co NPs after three extents of oxidation. The native sample has a thin (1.0 nm) CoO shell and exhibits no exchange biasing. The purposefully partially oxidized sample has a thicker CoO shell (3.2 nm), and is exchange biased. The sample fully oxidized to CoO loses exchange biasing. We observe three distinct magnetic properties that result from the finite-thickness antiferromagnet shell exchange coupled to a finite-size ferromagnet core, and from crystal and stoichiometric defects: (1) an enhancement of the thermal stability of the orientation of the magnetic moment due to exchange biasing in the partially oxidized sample, (2) a low-temperature paramagnetic response in the partially and fully oxidized samples due to defects in the CoO shell, and (3) an asymmetry in the field-dependent magnetization for the partially oxidized sample at low temperature due to small clusters of Co in a diffusion layer around the Co core. We propose a simple model to interpret these effects.

DOI: 10.1103/PhysRevB.72.064404 PACS number(s): 75.75.+a, 81.07.−b

I. INTRODUCTION

When a sample containing an interface between a ferromagnet (FM) and an antiferromagnet (AFM) is cooled in a magnetic field, it may exhibit an additional unidirectional anisotropy due to magnetic coupling at the interface. This effect, called exchange biasing (EB), was first discovered nearly 50 years ago in oxidized Co nanoparticles (NPs).[1] EB has been observed in many other magnetic materials, and vigorous experimental and theoretical research on EB continues. Although much progress has been made, the microscopic mechanism of EB still is not completely understood. Exchange-biased materials have important technological applications, such as in giant-magnetoresistance-based spin valves that are used in hard drive read heads; other spintronics applications, such as magnetic random access memory, are under development.[2] For further background on EB, we refer to recent reviews.[3–6]

The interface between Co (FM) and CoO (AFM) has been used as a prototype for studying EB because it has a large unidirectional anisotropy, and the ordering temperature of bulk CoO, the Néel temperature (T_N), is near room temperature at 293 K.[7] Above T_N, CoO is paramagnetic. Exchange-biased Co/CoO interfaces have been investigated in thin films[8] and NPs that have been prepared using cluster-beam deposition,[9] chemical vapor deposition,[10] sputtering,[11,12] and also colloidal methods.[13,14] Colloidal Co NPs can be economically prepared using wet chemical methods with a high level of control over NP size and crystal structure.[15–21] NP surface functionalization can be well controlled and exploited to manipulate[22] and assemble NPs[15,16,23] in ways that are not possible for particles prepared using physical methods. In particular, surface ligands control particle solubility, prevent agglomeration, and can provide functional groups for further chemistry on the NP surface.

In this paper, we report a systematic investigation of the magnetic properties of colloidal Co NPs after three extents of oxidation. The native sample has a thin (1.0 nm) CoO shell and exhibits no exchange biasing. The purposefully partially oxidized sample has a thicker CoO shell (3.2 nm), and is exchange biased. The sample fully oxidized to CoO loses exchange biasing. We observe three distinct magnetic properties that result from the finite-thickness antiferromagnet shell exchange coupled to a finite-size ferromagnet core, and from crystal and stoichiometric defects: (1) an enhancement of the thermal stability of the orientation of the magnetic moment due to exchange biasing in the partially oxidized sample, (2) a low-temperature paramagnetic response in the partially and fully oxidized samples due to defects in the CoO shell, and (3) an asymmetry in the field-dependent magnetization for the partially oxidized sample at low temperature due to small clusters of Co in a diffusion layer around the Co core.

II. EXPERIMENT

All of the NPs used in this study were prepared in the same batch in order to eliminate size variations among different batches. Co NPs were prepared as follows. In an inert atmosphere, 0.55 g $Co_2(CO)_8$ (Strem) was dissolved in 16 mL dioctyl ether (TCI). This solution was injected into a solution of 0.10 mL trioctlyphosphine (Strem, 97%) in 19 mL dioctyl ether at 235 °C. Following injection, the solution was heated at 180 °C for 10 min. The NPs began to aggregate, and 0.14 g stearic acid (Aldrich, 98%) was added. After heating the mixture for another 10 min at 180 °C, the NPs redispersed. The NPs were precipitated by adding ethanol, and were redispersed in tetrahydrofuran. They could be stored indefinitely in a nitrogen glovebox, but were found to have slightly oxidized. We identify this as the "native" sample. The sample that was purposefully partially oxidized was prepared by bubbling air through a solution of the native sample for 5 min and then waiting 6 weeks. To prepare the

sample that was fully oxidized to CoO, the NPs were transferred back into dioctyl ether and heated while bubbling air through the solution at 100 °C for 28 h. After each extent of oxidation, some NPs were dispersed in poly(lauryl methacrylate) cross-linked with ethyleneglycol dimethacrylate.[24] The NP concentration was chosen to be dilute so that the average interparticle distance was greater than 70 nm, a distance at which dipolar coupling between NPs is negligible. These NP-polymer samples were stored in a nitrogen glovebox in order to prevent further oxidation. Elemental analysis was performed on the polymer samples by Galbraith Laboratories, Inc., using inductively coupled plasma–optical emission spectroscopy.

Transmission electron microscopy (TEM) was performed on a JEOL 2000 FX microscope, and high-resolution TEM (HRTEM) was performed on a JEOL 2010. Superconducting quantum interference device (SQUID) measurements were performed on a Quantum Design MPMS-5S. In the M vs H measurements, a correction was made to remove the diamagnetic background of the polymer. The magnetization units of emu/g reported throughout this paper are based on the mass of cobalt. The mass of ligands and oxygen in the oxidized samples is excluded.

III. RESULTS AND DISCUSSION

TEM images of the native NPs [Fig. 1(a)] show that they have a diameter of 7.8 nm with a standard deviation of 1.0 nm. They are polycrystalline fcc with many defects, as seen in the "speckled" contrast in each NP. Partially oxidized NPs [Fig. 1(b)] are polycrystalline, but individual crystalline grains are resolvable. HRTEM micrographs show that these partially oxidized NPs are composed of grains of about 3 nm in diameter. Typically, there are one or two central grains surrounded by 4–7 grains in each NP. Many of the partially oxidized NPs show darkened cores, rather than the random distribution of dark spots that was observed for the native sample. These TEM images are similar to those in another study of partially oxidized NPs.[25]

The fully oxidized NPs [Fig. 1(c)] are polycrystalline and hollow, which is consistent with a similar recent study performed on single-crystal ε-Co NPs.[26] The outer diameter of the NPs has increased to accommodate the hollow cavity and the volume expansion as oxygen was incorporated into the NPs. Using electron diffraction (Fig. 2), the crystal structure of the oxide phase after heating in air was verified to be CoO. A more thermodynamically stable oxide phase is Co_3O_4, but a higher heating temperature is generally required to prepare it.[27] CoO has a rocksalt crystal structure, whereas Co_3O_4 is spinel. Each ring was assigned to CoO as follows: $A \sim \langle 111 \rangle; B \sim \langle 200 \rangle; C \sim \langle 220 \rangle; D \sim \langle 311 \rangle$ and $\langle 222 \rangle$; $E \sim \langle 400 \rangle; F \sim \langle 331 \rangle$ and $\langle 420 \rangle; G \sim \langle 422 \rangle$. No additional rings were observed. If the sample were Co_3O_4, no $\langle 200 \rangle$, $\langle 331 \rangle$, and $\langle 420 \rangle$ reflections would be observed, but these reflections were observed and are attributed to CoO. Furthermore, if a significant amount of Co_3O_4 were present, its $\langle 111 \rangle$ and $\langle 220 \rangle$ planes would give rise to rings inside of A, but because no rings were observed inside of A, the absence of the $\langle 111 \rangle$ and $\langle 220 \rangle$ reflections also shows that Co_3O_4 is not significantly present.

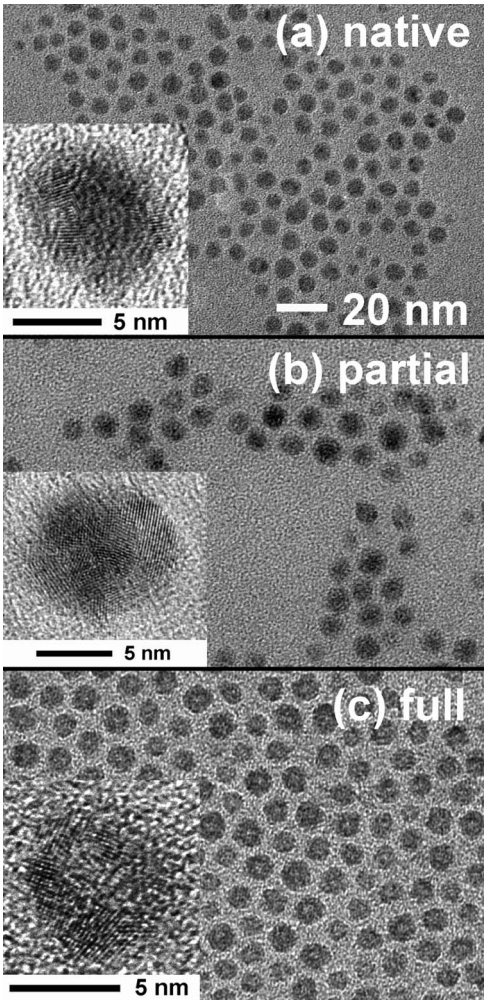

FIG. 1. TEM and HRTEM (insets) of Co NPs with (a) native, (b) partial, and (c) full oxidation.

The M vs H curves for native NPs after cooling in a 5 T field [Fig. 3(a)] exhibit no exchange shift (H_{EB}). Although the Co cores are highly polycrystalline, they are too small to sustain domain walls and are single-domain magnets. We

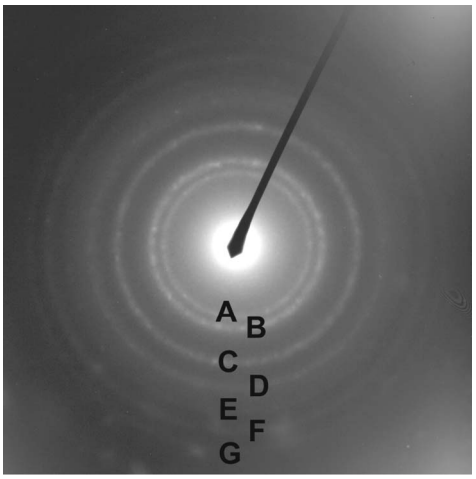

FIG. 2. Electron diffraction micrograph of product after heating native Co NPs in air at 100 °C for 28 h.

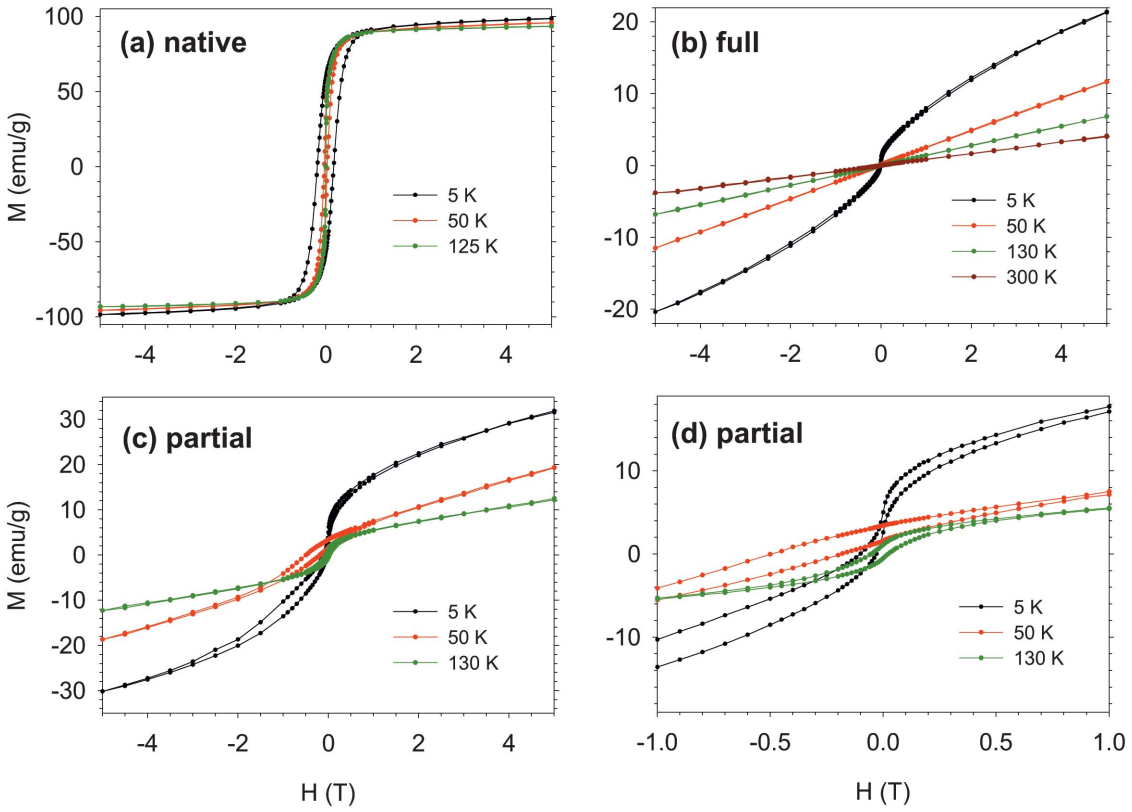

FIG. 3. (Color) Co NPs with (a) native, (b) full, and (c), (d) partial oxidation: M vs H after cooling from 300 K in a 5 T field at different temperatures. For clarity, data for (b), (c), and (d) at $T=25$, 100, 180, and 210 K, and for (c) and (d) at 300 K are omitted.

note that at high fields, the M vs H curves for native NPs do not exactly overlap, and an additional component with positive slope that is greatest at low temperature is observed, which is caused by the susceptibility of the CoO shell [Fig. 3(b)]. We used the M vs H curves for fully oxidized NPs to subtract the component of the temperature-dependent susceptibility of CoO, with which we calculated that M_S in the native sample is 91 emu/g. This value of M_S is 56% of the bulk magnetization for Co (162 emu/g).[28] Although interactions with carboxylate ligands that are chemisorbed[29] on the surface and residual CO from the NP preparation could reduce M_S below the bulk value,[18,30–32] these effects cannot explain such a large reduction, and we conclude that the reduction of M_S must be primarily caused by the formation of a thin layer of CoO on the surface of our native NPs, the thickness of which we measure later in the paper.

The product of the magnetocrystalline anisotropy constant (K) times the volume (V) is $KV=k_BT_B\ln(\omega_0/\omega)$, where T_B is the blocking temperature, ω is the measurement frequency, and we set $\omega_0=10^9$ Hz.[33] Cobalt is ferromagnetic when $T<T_B$, and for $T>T_B$ it is superparamagnetic. In this study, we measure the blocking temperature of the Co moments and do not directly measure moments of CoO grains because they are antiferromagnetic and their crystal axes are randomly oriented, but CoO grains also have a blocking temperature ($T_{B,\mathrm{CoO}}$) above which they are superparamagnetic. The blocking temperature of the Co moments is measured experimentally as the temperature at which there is a peak in the zero-field-cooled (ZFC) temperature-dependent magnetization for dc measurements, or in the in-phase susceptibility (χ') for ac measurements. From ac measurements of the slightly oxidized sample at a frequency of 1 kHz, we measured $T_B=195$ K and calculated the product $KV=3.7\times10^{-20}$ J.

In dc measurements of the native sample [Fig. 4(a)], we found that T_B of the Co is 120 K. Since T_B is linearly proportional to V, we can propagate the standard deviation of the diameter distribution as measured by TEM into a standard deviation of 43 K in T_B. The effect of the size distribution is to make the peak in Fig. 4(a) broader than it would be if the NPs were perfectly monodisperse. After oxidizing the sample to form partially oxidized NPs [Fig. 4(b)], T_B of the Co core increases to 170 K. For the fully oxidized sample [Fig. 4(c)], there is no peak that corresponds to a ferromagnetic core becoming superparamagnetic, which indicates that oxidation was complete. The moments of the Co cores before and after partial oxidation were measured using the Curie-Weiss law by fitting a line to the ZFC $1/M$ vs T curve for $T>T_B$ in Figs. 4(a) and 4(b), which is a standard analysis procedure. The value of the slope extracted from $1/M$ vs T was multiplied by a factor of 0.56 in order to account for the oxide shell on the native sample and to normalize the units of M to be emu/g of unoxidized Co. In order to relate the moment of the ferromagnetic core of the particles to its volume, we used the bulk M_S (162 emu/g).

The average moment per native NP (m_{native}) was $30\,700\mu_B$, which corresponds to a Co core diameter of 7.2 nm. We can now estimate an upper limit of the CoO thick-

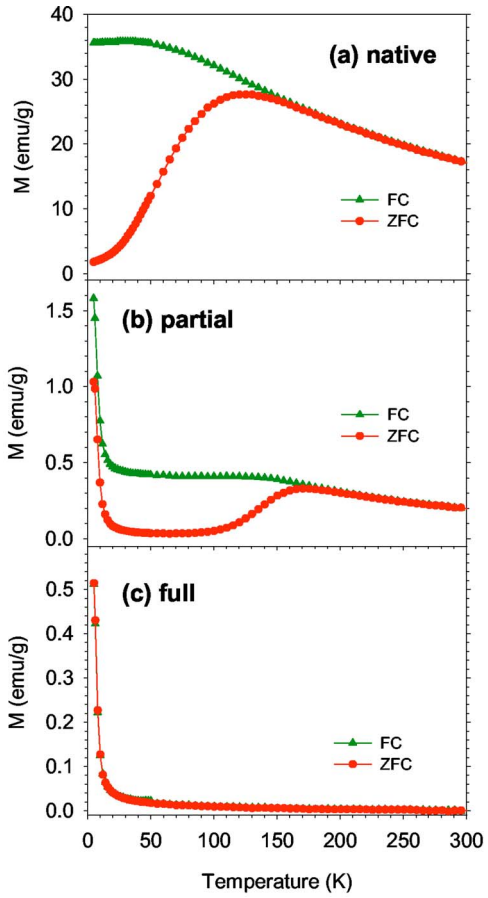

FIG. 4. (Color online) Co NPs with (a) native, (b) partial, and (c) full oxidation: M vs T for ZFC and field-cooled (FC) samples measured in 0.01 T field.

ness. After correcting for density differences in the Co core and CoO shell, we find that if 56% of the Co atoms are in the core, then the oxide thickness is ~1.0 nm, which gives a total native NP diameter of ~9.2 nm. Using this diameter, we find $K=9.1\times10^4$ J/m^3(9.1×10^5 erg/cm^3) from the product KV, which is consistent with values from other measurements of polycrystalline fcc NPs.[34] We note that the total diameter measured from these SQUID measurements is slightly larger than that measured from TEM. TEM measurements may tend to slightly underestimate NP sizes, since it can be difficult to observe surface layers in TEM. Because the NPs were briefly heated in air when preparing polymer sticks, it is also possible that the native NPs that were measured in the SQUID had slightly more oxide and thus a larger diameter than those that were viewed in TEM.

For the partially oxidized NPs, the moment of the core determined from Curie-Weiss analysis ($m_{partial}$) was $2900\mu_B$. If we assume, as expected, that the moment scales linearly with the volume of the Co domain, then the Co core diameter in the partially oxidized NPs is 3.3 nm, and the oxide thickness is 3.2 nm. Even though the size of the Co core has decreased in the partially oxidized NPs, T_B has increased due to EB on each NP, which increases the effective anisotropy. Since T_B scales linearly with volume, if K is assumed to be independent of size, then T_B of the Co core of the partially oxidized NPs without any oxide would be 11 K, which strongly underscores the enhanced thermal stability provided by the CoO shell. A similar increase in T_B due to EB has been observed previously for sputtered Co NPs in a bulk CoO matrix.[11]

Because EB occurs only for $T<T_N$, the upper limit of the temperature at which EB may be observed is T_N. However, for finite-thickness antiferromagnets, the anisotropy enhancement of EB can vanish at temperatures significantly below T_N.[35,36] In order for EB to occur, the AFM must be able to pin the FM as it is reversed. A couple of mechanisms by which small AFM grains may fail to pin an adjacent FM as the temperature increases are (1) if the AFM becomes superparamagnetic above a blocking temperature $T_{B,\mathrm{CoO}}<T_N$, or (2) if the magnetocrystalline anisotropy of CoO decreases so that moments throughout a domain in the AFM would all rotate as the FM moment reverses.[10] Although our experiments do not elucidate the mechanism of EB, the oxide layer on the native NPs is too thin for the sample to exhibit EB at any temperature, which others have also reported.[11] For partially oxidized NPs, however, EB causes T_B of the Co core to increase to 170 K. $T_{B,\mathrm{CoO}}$ provides an upper bound of the temperature to which EB can be used to stabilize the orientation of the magnetic moment of Co NPs. If the CoO grain size is increased, EB should stabilize the moments to a higher temperature, since both $T_{B,\mathrm{CoO}}$ and the magnetocrystalline anisotropy energy increase as the grain size increases.[37]

We sought a value of $T_{B,\mathrm{CoO}}$ for 3.2 nm CoO grains for comparison, but such a value is not consistently found in the thin film literature. The values reported for thin films of CoO with 3.0 nm thicknesses range from 170 (Ref. 38) to ~250–275 K.[35,37,39] These differences can most likely be attributed to differences among the microstructures of the films and different materials on which the CoO films are deposited. In particular, if the film is deposited on a ferromagnet or on a ferrimagnet, the exchange coupling at the interface may also change and have an effect in determining $T_{B,\mathrm{CoO}}$. From our experiments, we know that $T_{B,\mathrm{CoO}}\geqslant170$ K for our 3.2 nm grains, since EB is observed up to this temperature. Reported values of the magnetocrystalline anisotropy constant of CoO also vary widely with reports including $K_{\mathrm{CoO}}=5\times10^5$ J/m^3 (5×10^6 erg/cm^3) (Ref. 1) and $K_{\mathrm{CoO}}=1.1\times10^7$ J/m^3 (1.1×10^8 erg/cm^3).[35] These inconsistencies may also be due to microstructural differences and different measurement temperatures. If we assume that the grains are spheres of diameter 3.2 nm, we calculate $K_{\mathrm{CoO}}\geqslant3\times10^6$ J/m^3(3×10^7 erg/cm^3) from the expression $K_{\mathrm{CoO}}=k_BT_{B,\mathrm{CoO}}\ln(\omega_0/\omega)/V$, where we have used $\omega=0.01$ Hz, which is a value typically used for the time scale of dc SQUID measurements.

We now turn to our observation of a low-temperature paramagnetic response in the partially and fully oxidized samples which we attribute to defects in the CoO shell. Both samples exhibit a rise in the ZFC M vs T curve as T approaches zero [Figs. 4(b) and 4(c)]. This rise has previously been attributed to moments at defect sites in the CoO,[7] such as crystal defects at NP surfaces, grain boundaries, and variations in the Co to O stoichiometry. The moments associated with these crystal defects appear as paramagnetic impurities

because they are prevented from strongly coupling into the AFM lattice. In order to measure the moments associated with these defects, Curie-Weiss law analysis was performed by fitting a line to the ZFC $1/M$ vs T data for $T<50$ K in Figs. 4(b) and 4(c), which is the same procedure that we performed earlier for the Co cores. The moment per NP of the paramagnetic impurities in the CoO shell is $420\mu_B$ in the partially oxidized sample and $330\mu_B$ in the fully oxidized sample. If each defect is a Co^{2+} ion, which has a moment of $3.8\mu_B$,[40] then these measured moments correspond to about 95 Co^{2+} moments in the CoO shell that are not exchange coupled to the CoO lattice.

The assignment of these paramagnetic impurities as defects in the CoO shell is confirmed since these impurities were not observed in pure Co, and the moments are about the same in the partially and fully oxidized samples. Such impurities have also been observed in CoO thin films.[7] These defect moments may also have a significant effect on EB.[41] These quantitative measurements may also be useful for comparison with theoretical simulations of the properties of antiferromagnetic NPs.[42]

The M vs H curves for partially oxidized NPs [Figs. 3(c) and 3(d)] are rich with many phenomena, because this sample has a FM core and AFM shell and exhibits EB. Before considering the asymmetries in the M vs H measurements for partially oxidized NPs at low temperature, we first consider M vs H measurements for fully oxidized NPs [Fig. 3(b)], so that the component of the magnetization due to the CoO shell can be removed from the magnetization of the partially oxidized sample, which simplifies the analysis. The M vs H measurements for fully oxidized NPs [Fig. 3(b)] are linear for $T\geqslant 50$ K. At 5 K, the M vs H curve has a small positive shift along the magnetization axis and a superparamagnetic component. We are continuing to investigate the origin of this magnetization shift and superparamagnetic component, and we believe they are associated with the defect moments. We attribute the linear susceptibility, which is the dominant component of the M vs H curves, to Co^{2+} moments in the CoO lattice which cant away from the easy axis of the AFM lattice and into the field direction. Saturation does not occur for the partially or fully oxidized sample because CoO has a large magnetocrystalline anisotropy. If all the Co^{2+} moments could be aligned ferromagnetically, the resulting saturation magnetization for pure CoO would be 238 emu/g,[38] and even in a 5 T field, the magnetization does not approach saturation. The magnetic susceptibility of fully oxidized NPs decreases with increasing T, as the grains become superparamagnetic and then paramagnetic for $T>T_N$. There have been a few studies of the magnetic properties of CoO NPs,[43–45] but the magnetic measurements were performed only at room temperature, and the smallest particles studied had $d=15$ nm, for which $T_{B,\mathrm{CoO}}$ is not significantly reduced from the bulk value.[37]

A M vs H curve for the partially oxidized NPs from which the susceptibility contribution from CoO has been removed is shown in Fig. 5(a). In order to remove the susceptibility contribution of the CoO shell and consider only the core magnetization, EB, and other interface effects in the partially oxidized sample, we have subtracted M_{full} [Fig. 3(b)] multiplied by 0.947 from the curve for $M_{partial}$ [Fig. 3(c)]. This factor of 0.947 is derived as $1-[(m_{partial}/m_{native})/((91\ \mathrm{emu/g})/(162\ \mathrm{emu/g}))]$, because the partially oxidized NPs are not completely oxidized. The low-temperature behavior of the partially oxidized NPs exhibits many unusual properties.

(1) M_S of the Co core increases significantly as the temperature is lowered [Fig. 5(a)]. This is contrary to the expectation that M_S should be independent of temperature in this range.

(2) H_{EB} and H_C appear to be suppressed.

(3) The M vs H curve splits into two highly asymmetric lobes.

Each of these observations is explained using a simple model. The curve in Fig. 5(a) at 5 K is modeled as the sum of two curves [Fig. 5(b)]. The first curve simulates an exchange-biased Co core that has nonzero H_{EB} and H_C and is generated by shifting two Langevin functions along the H axis. The second curve is a Langevin function centered at the origin, which corresponds to a superparamagnet. The parameters for these curves were determined by fitting the model to experimental data. This simple model fits the data quite well.

The model reproduces property 1 well at each temperature, but the parameters from the fit change substantially at each temperature. As the temperature is increased to 300 K, we expect H_{EB} and H_C in the curve corresponding to the Co core to become smaller but for M_S to remain constant. In order for the superparamagnetic curve to fit the data, M_S decreases quickly with increasing temperature. Therefore, at a given temperature, this model works quite well, but the temperature-dependent M_S of the superparamagnetic curve decreases much more quickly than the flattening that occurs in a Langevin function as T increases.

Properties 2 and 3 are also reproduced well. The superparamagnetic curve that is only significant at low T splits the curve at 5 K into two lobes. EB is not suppressed, but the measured H_{EB} is reduced because the large lobe does not significantly intersect the field axis. If the fitting procedure is used to remove the superparamagnetic component, then H_{EB} as measured from the curve for the simulated exchange-biased core is 0.70 T at 5 K. We have repeated this fitting procedure at different temperatures, and have plotted H_{EB} and H_C from the curve for the simulated exchange biased core [Fig. 5(b), inset]. We find that H_{EB} and H_C decrease with increasing T and vanish when $T>T_{B,\mathrm{Co}}$, as is expected.

We propose that there are clusters of a few unoxidized Co atoms in a Co-rich, O-deficient diffusion zone between the core and shell in the partially oxidized sample that are superparamagnetic at 5 K. We have already discussed measurements of paramagnetic defect moments in the CoO shell, which is a separate effect. For these clusters, M_S may decrease with increasing temperature because they are very small, and their surfaces are exchange coupled to the surrounding CoO spins, which could cause them to violate the Langevin temperature dependence, thus explaining property 1. As evidence for such Co clusters, we note that the height of the low-temperature rise in the ZFC magnetization of the partially oxidized sample [Fig. 4(b)] is 1.0 emu/g, but it is only 0.5 emu/g for the fully oxidized sample [Fig. 4(c)]. This difference suggests that there are additional superparamagnetic spins at low temperature in the partially oxidized

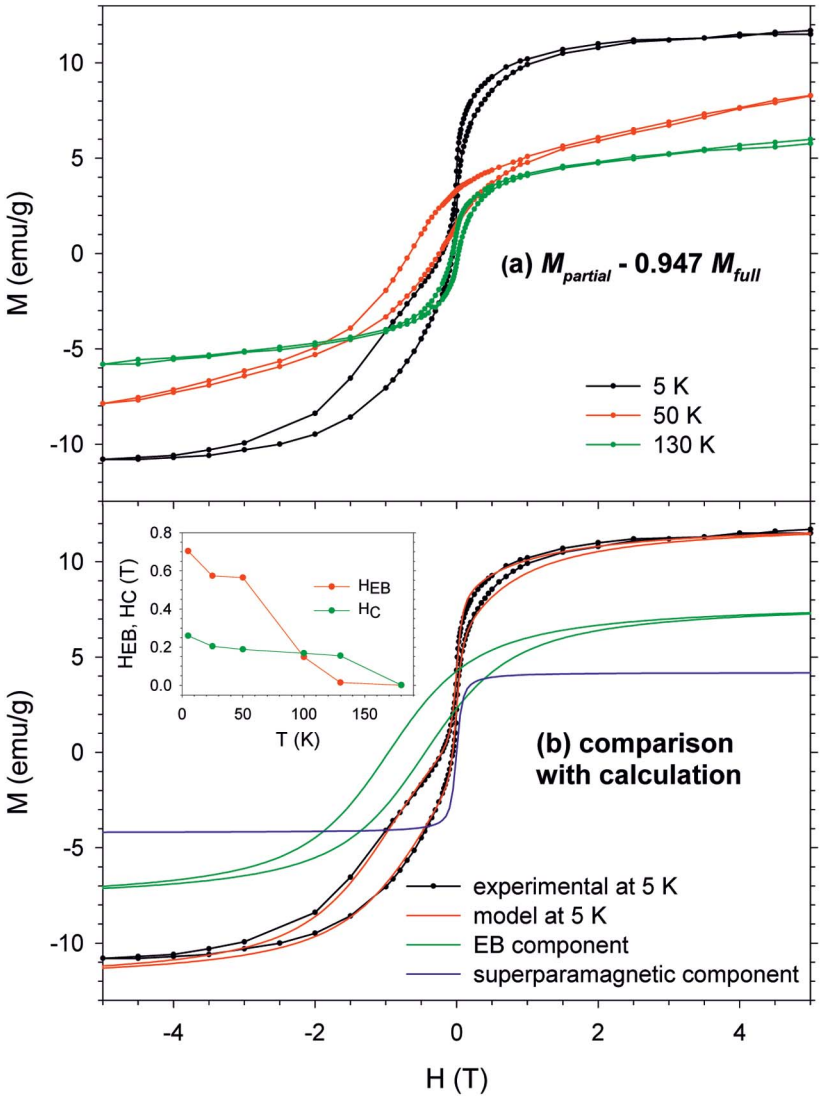

FIG. 5. (Color) M vs H for the partially oxidized sample after subtracting 0.947 times M_{full}: (a) from experimental data and (b) compared with modeled curves at 5 K; inset, H_{EB} and H_C vs T.

sample. A similar physical model of small ferromagnetic clusters at a metal/oxide interface was also recently proposed for the surfaces of FePt NPs.[46] Our model may also be applicable to work on α-Fe(core)/γ-Fe_2O_3(shell) NPs, in which a M vs H curve with a similar asymmetry to ours was observed at low temperature.[47]

Most other physical explanations for the superparamagnetic curve that we considered are inconsistent with the model. The superparamagnetic curve cannot be due to Co cores that are not significantly oxidized because M_S quickly decays with increasing temperature, which is inconsistent with the Langevin behavior that unoxidized cores would exhibit. One might attribute the superparamagnetic curve to an interaction between the Co core and CoO shell, such as moments in CoO canting about the field of the core, or of defect moments orienting in the field generated by the core. Such an explanation is not plausible because the superparamagnetic curve is symmetric about zero field and does not follow the exchange biased curve, as one would expect for an interaction with the cores. The superparamagnetic curve must be caused by an interaction with the applied field. Moreover, the magnetization of the CoO shell has already been removed in Fig. 5(a), so the superparamagnetic curve cannot be attributed to an interaction between the applied field and the defect moments present in the CoO shell for both the partially and fully oxidized samples.

IV. PROPOSAL

It has previously been suggested that the enhancement in the thermal stability of magnetic NPs caused by EB could be useful for developing high-density magnetic recording media.[11] A challenge in developing high-density magnetic recording media is that as the ferromagnetic NP size decreases, T_B also decreases, but useful media must be operable at room temperature. In order to increase the thermal stability of magnetic NPs, their magnetic anisotropy must be increased. Colloidally prepared FePt NPs are actively being pursued as a potential material for high-density magnetic recording due to their high magnetocrystalline anisotropy.[48] However, the desirable high-anisotropy, high-coercivity phase of FePt is achieved only after annealing, which leads to sintering and agglomeration,[46,49,50] thereby causing a polydisperse size distribution and inhomogeneous magnetic properties.

In order to use EB rather than intrinsically high magneocrystalline anisotropy, a pair of FM-AFM materials could be chosen that exhibit EB, and for which the AFM has T_N and $T_{B,AFM}$ sufficiently greater than room temperature. Colloidal NPs of the FM could be patterned on a substrate. These NPs would be superparamagnetic when not coupled to the AFM. After removing the ligands, a thin film of the AFM could then be deposited. By cooling the substrate below T_N in a field, the unidirectional anisotropy directions of all of the NPs would be oriented in the same direction.

This approach would circumvent the challenges associated with preparing the high-coercivity phase of FePt NPs and would also solve the problem of aligning the anisotropy axes of all the NPs into the same direction. However, we expect that the high coercivity of exchange biased bits that are stable at room temperature would likely cause them to be unwritable using today's write-head technology.[51] Advances in both media and head technology are necessary for developing usable magnetic media with higher bit densities.

V. CONCLUSIONS

In conclusion, we have comprehensively investigated the magnetic properties of colloidal Co NPs with native, partial, and full oxidation. Beyond a minimum CoO shell thickness, EB greatly enhances the anisotropy of Co NPs and stabilizes their magnetic moments to higher temperatures. A phenomenological model was developed to describe the unusual M vs H curves for partially oxidized NPs at low T. We attribute these unusual magnetic properties to clusters of Co atoms in a diffusion region at the interface in partially oxidized NPs. Paramagnetic spins at defect sites in CoO were also quantitatively measured.

ACKNOWLEDGMENTS

We thank Young Lee and Bob O'Handley for helpful discussions. We also gratefully acknowledge Fangcheng Chou for training on the SQUID magnetometer and Mike Frongillo for training on TEM. This work was supported by the NSF-NSEC at Harvard, the NSF-MRSEC at MIT, a NSF-NIRT grant, and the Packard Foundation. J.B.T. acknowledges support from the U.S. DOD, and D.N.W. acknowledges support from the German DAAD.

*Author to whom correspondence should be addressed.

[1] W. H. Meiklejohn and C. P. Bean, Phys. Rev. **105**, 904 (1957).
[2] S. A. Wolf, D. D. Awschalom, R. A. Buhrman, J. M. Daughton, S. von Molnár, M. L. Roukes, A. Y. Chtchelkanova, and D. M. Treger, Science **294**, 1488 (2001).
[3] A. E. Berkowitz and K. Takano, J. Magn. Magn. Mater. **200**, 552 (1999).
[4] J. Nogués and I. K. Schuller, J. Magn. Magn. Mater. **192**, 203 (1999).
[5] M. Kiwi, J. Magn. Magn. Mater. **234**, 584 (2001).
[6] R. L. Stamps, J. Phys. D **33**, R247 (2000).
[7] K. Takano, R. H. Kodama, A. E. Berkowitz, W. Cao, and G. Thomas, Phys. Rev. Lett. **79**, 1130 (1997).
[8] F. Radu, M. Etzkorn, R. Siebrecht, T. Schmitte, K. Westerholt, and H. Zabel, Phys. Rev. B **67**, 134409 (2003).
[9] D. L. Peng, K. Sumiyama, T. Hihara, S. Yamamuro, and T. J. Konno, Phys. Rev. B **61**, 3103 (2000).
[10] S. Gangopadhyay, G. C. Hadjipanayis, C. M. Sorensen, and K. J. Klabunde, J. Appl. Phys. **73**, 6964 (1993).
[11] V. Skumryev, S. Stoyanov, Y. Zhang, G. Hadjipanayis, D. Givord, and J. Nogués, Nature (London) **423**, 850 (2003).
[12] R. Morel, A. Brenac, and C. Portemont, J. Appl. Phys. **95**, 3757 (2004).
[13] M. Verelst, T. O. Ely, C. Amiens, E. Snoeck, P. Lecante, A. Mosset, M. Respaud, J. M. Broto, and B. Chaudret, Chem. Mater. **11**, 2702 (1999).
[14] M. Spasova, U. Wiedwald, M. Farle, T. Radetic, U. Dahmen, M. Hilgendorff, and M. Giersig, J. Magn. Magn. Mater. **272-276**, 1508 (2004).
[15] S. Sun and C. B. Murray, J. Appl. Phys. **85**, 4325 (1999).
[16] V. F. Puntes, K. M. Krishnan, and P. Alivisatos, Appl. Phys. Lett. **78**, 2187 (2001).
[17] J.-K. Lee and S. M. Choi, Bull. Korean Chem. Soc. **24**, 32 (2003).
[18] J. Osuna, D. deCaro, C. Amiens, B. Chaudret, E. Snoeck, M. Respaud, J. M. Broto, and A. Fert, J. Phys. Chem. **100**, 14571 (1996).
[19] J. P. Chen, C. M. Sorensen, K. J. Klabunde, and G. C. Hadjipanayis, J. Appl. Phys. **76**, 6316 (1994).
[20] C. Petit and M. P. Pileni, J. Magn. Magn. Mater. **166**, 82 (1997).
[21] D. P. Dinega and M. G. Bawendi, Angew. Chem., Int. Ed. **38**, 1788 (1999).
[22] C. M. Niemeyer, Angew. Chem., Int. Ed. **40**, 4128 (2001).
[23] Y. Lalatonne, J. Richardi, and M. P. Pileni, Nat. Mater. **3**, 121 (2004).
[24] J. Lee, V. C. Sundar, J. R. Heine, M. G. Bawendi, and K. F. Jensen, Adv. Mater. (Weinheim, Ger.) **12**, 1102 (2000).
[25] M. Spasova, T. Radetic, N. S. Sobal, M. Hilgendorff, U. Wiedwald, M. Farle, M. Giersig, and U. Dahmen, in *Magnetic and Electronic Films–Microstructure, Texture and Application to Data Storage*, edited by P. W. DeHaven, D. P. Field, S. D. Harkmess IV, J. A. Sutliff, J. A. Szpunar, L. Tang, T. Thomson, and M. D. Vaudin, MRS Symposia Proceedings No. 721 (Materials Research Society, Pittsburgh, 2002), p. 195.
[26] Y. Yin, R. M. Rioux, C. K. Erdonmez, S. Hughes, G. A. Somorjai, and A. P. Alivisatos, Science **304**, 711 (2004).
[27] N. N. Greenwood and A. Earnshaw, in *Chemistry of the Elements* (Butterworth-Heinemann, Boston, 1997).
[28] R. C. O'Handley, *Modern Magnetic Materials: Principles and Applications* (John Wiley & Sons, New York, 2000).
[29] N. Wu, L. Fu, M. Su, M. Aslam, K. C. Wong, and V. P. Dravid, Nano Lett. **4**, 383 (2004).
[30] Š. Pick and H. Dreyssé, Phys. Rev. B **59**, 4195 (1999).
[31] A. E. Berkowitz, J. A. Lahut, I. S. Jacobs, L. M. Levinson, and D. W. Forester, Phys. Rev. Lett. **34**, 594 (1975).
[32] C. M. Sorensen, in *Nanoscale Materials in Chemistry*, edited by

K. J. Klabunde (Wiley-Interscience, New York, 2001), p. 169.
[33] S. Blundell, *Magnetism in Condensed Matter* (Oxford University Press, New York, 2001).
[34] G. A. Held, G. Grinstein, H. Doyle, S. Sun, and C. B. Murray, Phys. Rev. B **64**, 012408 (2001).
[35] P. J. van der Zaag, Y. Ijiri, J. A. Borchers, L. F. Feiner, R. M. Wolf, J. M. Gaines, R. W. Erwin, and M. A. Verheijen, Phys. Rev. Lett. **84**, 6102 (2000).
[36] U. Nowak, K. D. Usadel, J. Keller, P. Miltényi, B. Beschoten, and G. Güntherodt, Phys. Rev. B **66**, 014430 (2002).
[37] Y. J. Tang, D. J. Smith, B. L. Zink, F. Hellman, and A. E. Berkowitz, Phys. Rev. B **67**, 054408 (2003).
[38] T. Ambrose and C. L. Chien, Phys. Rev. Lett. **76**, 1743 (1996).
[39] E. N. Abarra, K. Takano, F. Hellman, and A. E. Berkowitz, Phys. Rev. Lett. **77**, 3451 (1996).
[40] W. L. Roth, Phys. Rev. **110**, 1333 (1958).
[41] J. Keller, P. Miltényi, B. Beschoten, G. Güntherodt, U. Nowak, and K. D. Usadel, Phys. Rev. B **66**, 014431 (2002).
[42] R. H. Kodama and A. E. Berkowitz, Phys. Rev. B **59**, 6321 (1999).
[43] L. Zhang, D. Xue, and C. Gao, J. Magn. Magn. Mater. **267**, 111 (2003).
[44] L. Zhang and D. Xue, J. Mater. Sci. Lett. **21**, 1931 (2002).
[45] C. F. J. Flipse, C. B. Rouwelaar, and F. M. F. De Groot, Eur. Phys. J. D **9**, 479 (1999).
[46] T. Thomson, M. F. Toney, S. Raoux, S. L. Lee, S. Sun, C. B. Murray, and B. D. Terris, J. Appl. Phys. **96**, 1197 (2004).
[47] R. K. Zheng, G. H. Wen, K. K. Fung, and X. X. Zhang, J. Appl. Phys. **95**, 5244 (2004).
[48] S. Sun, C. B. Murray, D. Weller, L. Folks, and A. Moser, Science **287**, 1989 (2000).
[49] T. J. Klemmer, C. Liu, N. Shukla, X. W. Wu, D. Weller, M. Tanase, D. E. Laughlin, and W. A. Soffa, J. Magn. Magn. Mater. **266**, 79 (2003).
[50] H. Zeng, S. H. Sun, T. S. Vedantam, J. P. Liu, Z. R. Dai, and Z. L. Wang, Appl. Phys. Lett. **80**, 2583 (2002).
[51] D. Weller, A. Moser, L. Folks, M. E. Best, W. Lee, M. F. Toney, M. Schwickert, J. U. Thiele, and M. F. Doerner, IEEE Trans. Magn. **36**, 10 (2000).